ACS Chemical Neuroscience

Research Article

pubs.acs.org/chemneuro

NDE1 and GSK3β Associate with TRAK1 and Regulate Axonal Mitochondrial Motility: Identification of Cyclic AMP as a Novel Modulator of Axonal Mitochondrial Trafficking

Fumiaki Ogawa,[†] Laura C. Murphy, Elise L. V. Malavasi, Shane T. O'Sullivan, Helen S. Torrance, David J. Porteous, and J. Kirsty Millar*

University of Edinburgh Centre for Genomic and Experimental Medicine, MRC Institute of Genetics and Molecular Medicine, Crewe Road, Edinburgh, EH4 2XU, United Kingdom

Supporting Information

ABSTRACT: Mitochondria are essential for neuronal function, providing the energy required to power neurotransmission, and fulfilling many important additional roles. In neurons, mitochondria must be efficiently transported to sites, including synapses, where their functions are required. Neurons, with their highly elongated morphology, are consequently extremely sensitive to defective mitochondrial trafficking which can lead to neuronal ill-health/death. We recently demonstrated that DISC1 associates with mitochondrial trafficking complexes where it associates with the core kinesin and dynein adaptor molecule TRAK1. We now show that the DISC1 interactors NDE1 and GSK3β also associate robustly with TRAK1 and demonstrate that NDE1 promotes retrograde axonal mitochondrial movement. GSK3β is known to modulate axonal mitochondrial motility, although reports of its actual effect are conflicting. We show that, in our system, GSK3β promotes anterograde mitochondrial transport. Finally, we investigated the influence of cAMP elevation upon mitochondrial motility, and found a striking increase in mitochondrial motility and retrograde movement. DISC1, NDE1, and GSK3β are implicated as risk factors for major mental illness. Our demonstration that they function together within mitochondrial trafficking complexes suggests that defective mitochondrial transport may be a contributory disease mechanism in some cases of psychiatric disorder.

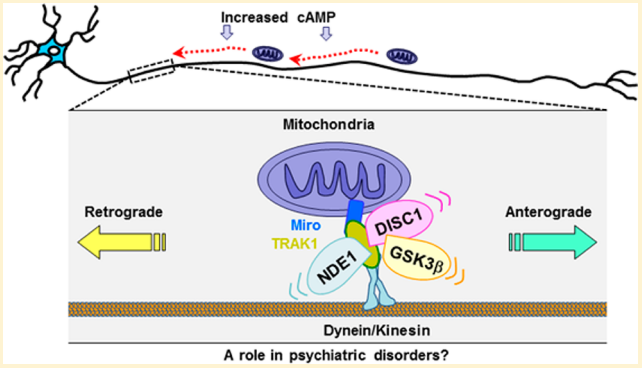

KEYWORDS: *Mitochondrial trafficking, TRAK1, NDE1, GSK3β: DISC1, cAMP*

Correct mitochondrial function is of paramount importance, to the brain, which accounts for approximately 20% of the body's energy consumption at rest.[1] Much of this energy consumption is due to neurosignaling processes, including neurotransmitter release into synapses, and re-establishment of ion gradients following depolarization.[1] To fulfill these and other functions, mitochondria are constantly trafficked around the cell.[1] Moreover, mitochondria undergo frequent fission and fusion events. Fusion is believed to facilitate transfer of factors between mitochondria, thus maintaining their health and optimum function.[2] This process is also dependent upon mitochondrial motility because mitochondria must be trafficked to meet before they can fuse. It follows that dysfunctional mitochondria and/or dysfunctional mitochondrial trafficking is tightly linked to brain disorder.[1] Neurons are particularly vulnerable to mitochondrial dysfunction and/or trafficking deficits on two counts, their intrinsic high energy demands, and their extremely extended morphology in comparison to other cell types, which demands efficient mobilization to the extremities.[2] Indeed, mitochondrial dysfunction/defective trafficking is believed to play a primary role in the pathology of several neurodegenerative diseases including Parkinson's disease, Huntington's disease, and Alzheimer's disease.[1]

Axonal mitochondrial trafficking involves TRAK1[3] which binds to the molecular motors kinesin and dynein,[4,5] and also interacts with Miro which is embedded in the outer mitochondrial membrane.[6] TRAK1 is thus a key molecule that connects mitochondria to their motors. We recently demonstrated a robust association between TRAK1 and DISC1 and, consistent with this, that DISC1 promotes anterograde mitochondrial transport.[7] DISC1 interacts with multiple additional proteins including the dynein regulators LIS1, NDE1, and NDEL1,[8−10] and the kinase GSK3β.[11]

Together with DISC1, NDE1 and GSK3β are of particular interest because they are relevant to psychiatry. *DISC1* is directly disrupted by a t(1;11) chromosomal translocation that is causally linked to major mental illness within a single Scottish family.[12,13] *NDE1* is targeted by recurrent genomic copy number variants

Received: September 28, 2015
Accepted: January 27, 2016
Published: January 27, 2016

DOI: 10.1021/acschemneuro.5b00255
ACS Chem. Neurosci. 2016, 7, 553−564

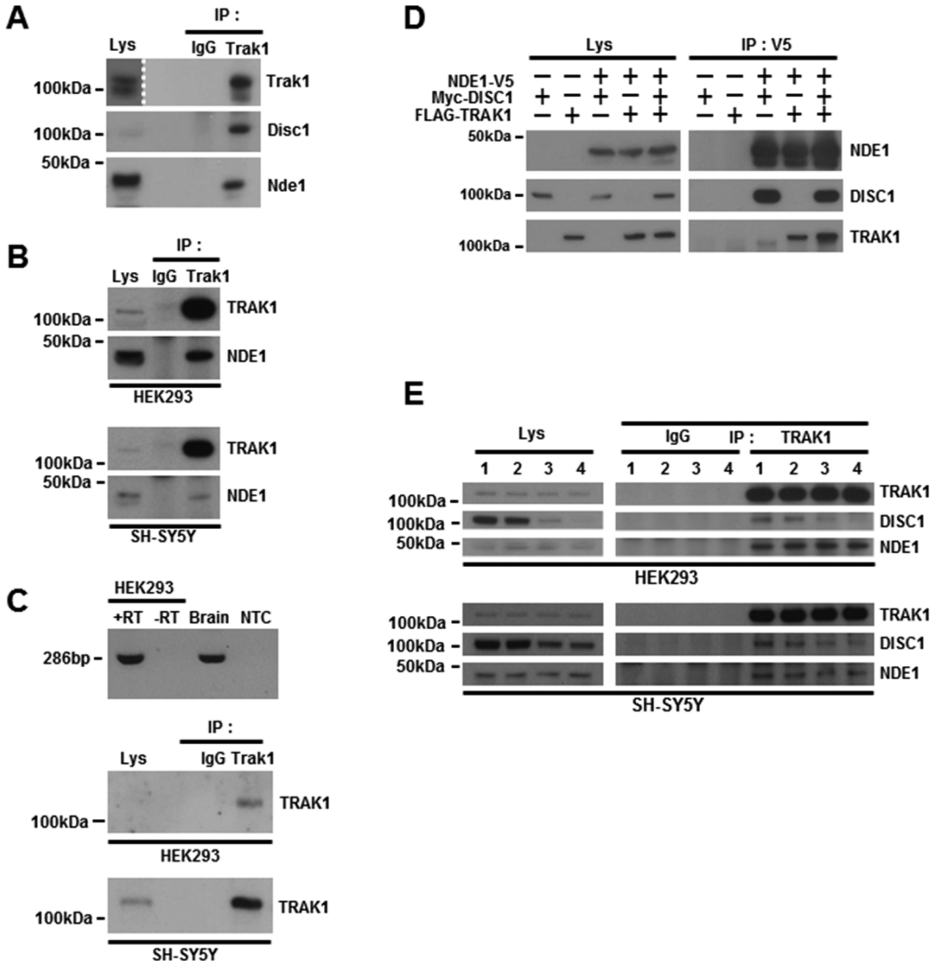

Figure 1. TRAK1 associates with NDE1 and LIS1. (A) Immunoprecipitation of Trak1 from adult mouse whole brain lysates co-immunoprecipitates Disc1 and Nde1. A longer exposure of the same immunoblot has been shown for the lysate Trak1 signal which was otherwise very weak. The dotted white line indicates the join between the superimposed longer exposure of the lysate track, and the shorter exposure for the other tracks. Trak1 was immunoprecipitated using an antibody from Santa Cruz Biotechnology and detected using an antibody from Sigma-Aldrich. (B) Immunoprecipitation of endogenous human TRAK1 from HEK293 (upper) and SH-SY5Y (lower) cell line lysates co-immunoprecipitates endogenous NDE1. Human TRAK1 was immunoprecipitated and detected using an antibody from Abcam. (C) Upper, amplification of TRAK1 transcripts from HEK293 cells using reverse transcriptase PCR and primers specific for TRAK1 exons 10 and 12. +RT, HEK293 cDNA template; −RT, minus reverse transcriptase negative control; brain, human brain cDNA positive control; NTC, no template negative control. Lower, an antibody specific for TRAK1 from Abcam immunoprecipitates endogenous human TRAK1 from SH-SY5Y cells and HEK293 cells. This immunoprecipitated TRAK1 cross-reacts with a TRAK1-specific antibody from Sigma, thus demonstrating the specificity of the Abcam antibody for TRAK1. Note that, although the HEK293 lysate TRAK1 signal is virtually undetectable here, the same lysate was used in Figure 4C where the TRAK1 signal is clearly visible. (D) Co-immunoprecipitation of exogenous Myc-DISC1 and FLAG-TRAK1 with NDE1-V5 from transfected COS7 cells. Absence of Myc-DISC1 does not abolish NDE1-V5/FLAG-TRAK1 co-immunoprecipitation. (E) DISC1 knockdown does not abolish co-immunoprecipitation of endogenous NDE1 with endogenous TRAK1 from HEK293 and SH-SY5Y cell line lysates. 1, mock transfection (no siRNA); 2, control siRNA; 3, siRNA targeting DISC1 exon 13; 4, siRNA targeting DISC1 exon 2.

that are more frequent in psychiatric patients than controls.[14] GSK3β is a major target of lithium chloride, a drug in clinical use as a mood stabilizer.[15,16] Moreover, *GSK3β* is targeted by genomic copy number variants that are more commonly found in psychiatric patients.[17] Studying functional complexes involving these proteins may therefore identify molecular mechanisms underlying psychiatric disorders.

The highly homologous orthologues NDE1 and NDEL1 cooperate with LIS1 in regulating dynein. NDEL1 promotes LIS1 binding to microtubules and, in turn, recruitment of dynein,[18] while NDE1 has been to shown to recruit LIS1 to dynein.[19] Although these mechanisms are incompletely understood, it is clear that dynein modulation involves LIS1 binding to NDE1 or NDEL1. Together these proteins control a number of functions requiring dynein force generation, leading to important roles in critical brain processes including neural precursor proliferation and neuronal migration.[20] Involvement in mitochondrial trafficking is now emerging as another important function. A role for Lis1 and Ndel1 in this process has previously been demonstrated.[21] Consistent with their role in activating the retrograde motor dynein,[18,19,22,23] knockdown of either Lis1 or Ndel1 inhibits retrograde mitochondrial movement in axons of rat hippocampal neurons.[21] Although these observations clearly demonstrate a role for the Lis1/Ndel1 complex in regulating the direction of mitochondrial movement, a role in this process has not been demonstrated until now for the highly homologous Ndel1 orthologue Nde1.

GSK3β is also known to regulate mitochondrial transport, although reports of the actual effect are somewhat conflicting. Chen et al. reported that inhibiting GSK3β increases

DOI: 10.1021/acschemneuro.5b00255
ACS Chem. Neurosci. 2016, 7, 553−564

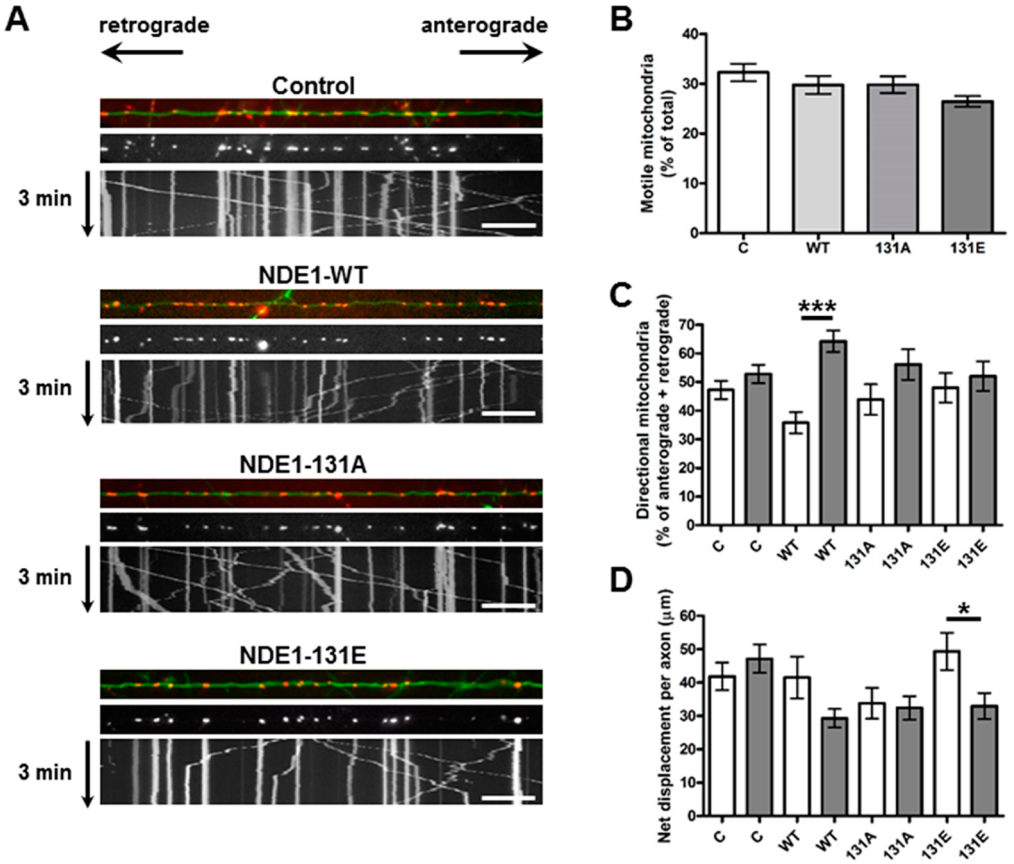

Figure 2. NDE1 overexpression promotes retrograde mitochondrial movement within axons of mouse hippocampal neurons. Cultured hippocampal neurons (DIV6−7) were cotransfected with GFP, DsRed2-mito and either empty vector (C), NDE1-V5 (WT), NDE1-131A (131A), or NDE1-131E (131E). Time-lapse imaging was performed 1 day post-transfection. (A) Representative images of axons and of kymographs. Scale bars: 20 μm. (B) Mitochondrial motility expressed as percentage of total mitochondria per axon. (C) Motile mitochondria moving in the anterograde (white) or retrograde (dark gray) direction expressed as percentage of anterograde plus retrograde mitochondria per axon. One-way ANOVA $p = 0.001$. (D) Average net mitochondrial displacement per axon of mitochondria moving in the anterograde (white) or retrograde (dark gray) direction. One-way ANOVA $p = 0.007$. $n = 7$ independent neuronal cultures. Error bars represent SEM $^*p < 0.05$, $^{***}p < 0.001$.

mitochondrial motility in cultured hippocampal neurons.[24] However, Llorens-Martin et al. found that GSK3β overexpression in cultured mouse hippocampal neurons increases axonal mitochondrial motility in both directions, but most robustly in the anterograde direction.[25] The mechanism by which these effects occur has been proposed to involve tau,[25] or modulation of tubulin acetylation by GSK3β[26] which, in turn, regulates kinesin-1 binding to microtubules.[27]

We hypothesized that DISC1, NDE1, GSK3β, and TRAK1 assemble in a molecular complex that directly participates in the regulation of mitochondrial trafficking in neurons. Here we show that Gsk3β and Nde1 associate robustly with Trak1. We demonstrate that NDE1 promotes retrograde mitochondrial movement when overexpressed within axons, an effect that is blocked by a phosphomimic mutation (NDE1-131E) that disrupts NDE1 interaction with LIS1.[28] We also show that GSK3β overexpression increases anterograde axonal mitochondrial motility, in partial agreement with a previous study.[25] These observations indicate that the emerging roles of NDE1/NDEL1 and GSK3β in regulation of mitochondrial trafficking are likely mediated by their incorporation into mitochondrial trafficking complexes built around TRAK1. Direct involvement of these interacting proteins, including DISC1, in mitochondrial trafficking suggests that this mechanism may be defective in some cases of psychiatric illness.

Finally, because phosphorylation of residue 131 in NDE1 is cAMP-dependent,[28] we investigated the effect of cAMP upregulation and observed a rapid elevation in the number of retrograde-moving axonal mitochondria. This indicates that cAMP is likely an important novel signal that guides axonal mitochondrial motility.

RESULTS AND DISCUSSION

Having previously demonstrated that endogenous DISC1 and TRAK1 associate in human cell lines,[7] we first wanted to show that DISC1 associates with TRAK1 in brain. To do this we immunoprecipitated endogenous mouse Trak1 from adult mouse brain lysates (Figure 1A). We used an in-house antibody specific for mouse Disc1 to demonstrate that a protein species of approximately 100 kDa, the size of full-length Disc1, is robustly co-immunoprecipitated with mouse Trak1 (Figure 1A). This antibody fails to detect any 100 kDa species in whole brain tissue from adult mice where Disc1 exons 2 and 3 have been knocked out,[29,30] and thus, we are confident of its specificity for mouse Disc1. Because DISC1 also interacts with NDE1, a molecule that regulates dynein-mediated intracellular trafficking, we speculated that NDE1 may complex with TRAK1 to regulate dynein-dependent motility. We therefore next used an antibody that recognizes mouse Nde1 to demonstrate that Nde1 also robustly co-immunoprecipitates with mouse Trak1 from adult mouse

DOI: 10.1021/acschemneuro.5b00255
ACS Chem. Neurosci. 2016, 7, 553−564

Table 1. Numbers of Axons and Mitochondria in Each Category for the NDE1 Mitochondrial Trafficking Experiment

	no. axons	total no.	no. stationary	no. motile	no. anterograde	no. retrograde	no. direction undetermined	avg % motility
control	26	651	445	206	94	108	4	32
NDE1-WT	27	644	451	193	68	123	2	30
NDE1-131A	28	678	475	203	82	117	4	30
NDE1-131E	27	631	463	168	78	88	2	26.5

brain lysates (Figure 1A). Mouse Disc1 and Nde1 also co-immunoprecipitate with Trak1 from mouse brain crude synaptosome fractions that contain intrasynaptosomal mitochondria[31] and from light membrane fractions (Figure 4A). We explored the association between TRAK1 and NDE1 further by co-immunoprecipitating the endogenous proteins from the human cell lines HEK293 and SH-SY5Y (Figure 1B). We used reverse transcriptase RT-PCR to confirm that HEK293 cells express TRAK1, and demonstrated that TRAK1 can be immunoprecipitated from both cell lines using a TRAK1-specific antibody (from Abcam) and detected in immunoprecipitates by an independent TRAK1-specific antibody (from Sigma), thus confirming the specificity of both antibodies (Figure 1C). We found that TRAK1 immunoprecipitation using the Abcam antibody robustly co-immunoprecipitates NDE1 from both HEK293 and SH-SY5Y cells (Figure 1B). V5-NDE1 also strongly co-immunoprecipitates FLAG-TRAK1 from COS7 cells, with or without exogenous Myc-DISC1 (Figure 1D). Following cotransfection of SH-SY5Y cells, C-terminally V5-tagged NDE1 is widely distributed throughout the cytoplasm in a punctate pattern, while FLAG-TRAK1 is concentrated in the perinuclear region, as is typical when this protein is overexpressed.[7] FLAG-TRAK1 is additionally present as cytoplasmic puncta (Figure 3E), and in some cells is organized in a filamentous distribution (Figure 3E). A proportion of V5-NDE1 clearly associates with FLAG-TRAK1 in the perinuclear region, along the filaments, and at cytoplasmic puncta (Figure 3E), providing additional evidence for an association between NDE1 and TRAK1. NDE1 thus associates robustly with TRAK1. Additional in vitro binding experiments will be required to determine whether this is due to direct interaction.

These observations suggested that DISC1 may help recruit its interactor NDE1 to TRAK1 complexes. To test this possibility, the endogenous TRAK1 immunoprecipitation experiments were repeated using HEK293 or SH-SY5Y cells transfected with siRNAs that efficiently knock down human DISC1 expression.[7] In these experiments, endogenous DISC1 was knocked down by both siRNAs, and this level of knock down had no effect upon TRAK1/NDE1 association (Figure 1E). The robust association between NDE1 and TRAK1 is therefore not dependent upon DISC1.

The association of TRAK1 with DISC1 and NDE1 implies a co-operative role for these proteins in intracellular trafficking events. TRAK1 and DISC1 are both known to participate in axonal mitochondrial trafficking,[3,7,32] as are the NDE1/DISC1 interactors LIS1 and NDEL1.[21] We therefore next examined the influence of NDE1 upon axonal mitochondrial trafficking by transfecting primary mouse hippocampal neurons with NDE1-V5 and carrying out time-lapse imaging of mitochondrial movements within axons over a period of 3 min (Figure 2A, Table 1, and Supporting Information Videos NDE1 Control and NDE1-WT). Overexpression of NDE1-V5 has no effect upon the proportion of moving mitochondria within axons in comparison to empty vector-transfected neurons (Figure 2B). When we examined directional movement, we found no difference between the proportion of anterograde or retrograde moving axonal mitochondria in empty-vector transfected neurons. This is consistent with the published literature,[2] and represents the normal baseline condition in healthy cultured neurons. In contrast, in axons of neurons overexpressing NDE1-V5, an average of 64% of motile mitochondria move in the retrograde direction, compared to an average 36% of anterograde mitochondria ($p < 0.001$, Figure 2C). NDE1 therefore promotes retrograde axonal mitochondrial movement, consistent with a previous demonstration that knockdown of the NDE1 orthologue Ndel1 inhibits retrograde mitochondrial movement,.[21] NDE1 overexpression may achieve this effect through dynein activation,[18,19,22,23] although, since NDE1 binds directly to dynein, it is also possible that NDE1 overexpression exerts its effects by recruiting dynein to the trafficking complex.

We have previously demonstrated[28] that NDE1 is phosphorylated by protein kinase A (PKA) at sites including threonine 131 (T131). The T131 phosphorylation site is located within the binding site for LIS1 and, when phosphorylated, reduces LIS1/NDE1 interaction.[28] This phosphorylation site also promotes NDE1 interaction with its orthologue NDEL1 and may influence the ability of NDE1 to multimerize.[28] Phosphorylation of this site is therefore predicted to have many functional consequences, including modulation of dynein processivity because interaction of NDE1, or its orthologue NDEL1, with LIS1 is believed to be required for activation of dynein.[18,19,22,23] Consequently we hypothesized that the T131 site modulates mitochondrial motility. To explore this possibility we examined the effect of mutating T131 to alanine (phosphodead) or glutamate (phosphomimic) upon axonal mitochondrial trafficking (Supporting Information Videos NDE1-131A and NDE1-131E). This analysis demonstrated that mutation of T131 to the phosphomimic residue glutamate abolishes the ability of NDE1 to promote retrograde mitochondrial movement (Figure 2C). The NDE1-131A mutant has an intermediate effect, promoting retrograde movement, but not to the same extent as wild type NDE1 (Figure 2C). These data indicate that promotion of retrograde mitochondrial movement by NDE1 requires an unmodified Threonine residue at position 131. Since it has previously been demonstrated that binding of NDE1, or its orthologue NDEL1, to LIS1 activates the retrograde motor dynein,[18,19,22,23] our data suggest that NDE1 may promote retrograde mitochondrial movement, at least in part, by activating dynein via LIS1 binding. Unexpectedly, we also observed that NDE1-131E increases the average net displacement of mitochondria in the anterograde direction in comparison to the retrograde direction, whereas in the presence of empty vector, wild type NDE1, or NDE1-131A, average net displacement is approximately equal in each direction ($p < 0.05$, Figure 2D, Table 1). This is consistent with the tug-of-war hypothesis of bidirectional transport, whereby the opposing forces of anterograde and retrograde motors are coordinately regulated to determine movement direction. It is conceivable that the 131E mutant, in failing to activate retrograde movement, may release a brake on anterograde motility, resulting in

DOI: 10.1021/acschemneuro.5b00255
ACS Chem. Neurosci. 2016, 7, 553−564

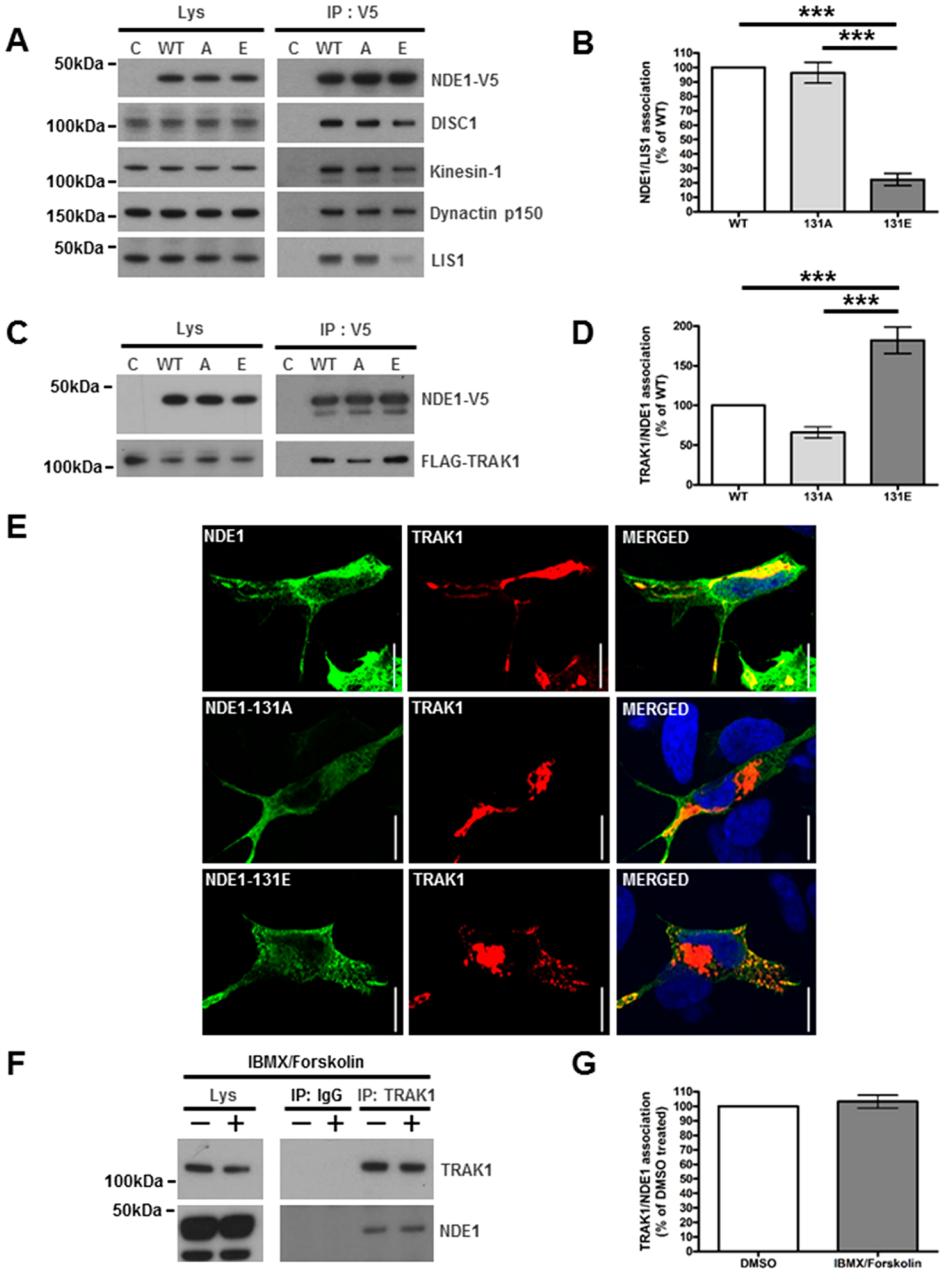

Figure 3. Effects of mutating the NDE1 T131 site. (A) SH-SY5Y cells were transfected with either empty vector (C), NDE1-V5 (WT), NDE1-131A-V5 (A), or NDE1-131E-V5 (E). Immunoprecipitations were then performed from lysates using a V5 antibody to examine co-immunoprecipitation of key NDE1 interactors. (B) Quantification of LIS1 co-immunoprecipitation by the V5 antibody from (A). One-way ANOVA $p < 0.0001$. $n = 5$. (C) SH-SY5Y cells were cotransfected with FLAG-TRAK1 and the V5-tagged forms of NDE1. Immunoprecipitations were carried out using the V5 antibody to determine the effect of mutating the T131 site upon FLAG-TRAK1 co-immunoprecipitation. (D) Quantification of TRAK1/NDE1 association from (C). One-way ANOVA $p < 0.0001$. $n = 5$. (E) Representative images demonstrating that V5-tagged NDE1, NDE1-131A, and NDE1-131E, detected using anti-NDE1 antibody (Proteintech), colocalize with FLAG-TRAK1, detected using anti-FLAG antibody, in cotransfected SH-SY5Y cells. Nuclei (blue) stained with Hoechst. Scale bars: 10 μm. (F) SH-SY5Y cells were treated with Forskolin (100 μM) plus IBMX (250 μM) to upregulate cAMP levels. Endogenous TRAK1 was immunoprecipitated to assess the effect of elevated cAMP concentration upon its association with NDE1. (G) Quantification of TRAK1/NDE1 association from (F). Error bars represent SEM. $n = 3$. ***$p < 0.001$.

increased movement of individual mitochondria in the anterograde direction.

To try to understand the mechanism underlying the effects of NDE1-T131 mutations upon mitochondrial motility, SH-SY5Y cells were transfected with the various forms of NDE1 to determine whether the 131 site influences NDE1 association with a number of endogenous proteins. Co-immunoprecipitation of endogenous kinesin-1 and dynactin p150 with NDE1-V5 is unaffected by mutation of the T131 site while, as expected,[28] NDE1-V5/LIS1 interaction is substantially reduced by the 131E mutation ($p < 0.001$, Figure 3A, B). The 131E phosphomimic therefore does not appear to influence the amount of NDE1-associated motor protein. There was also no effect upon NDE1/DISC1 association (Figure 3A). We therefore next examined whether the T131 site influences NDE1 association with TRAK1. In co-immunoprecipitation experiments using COS7 cells, there was little effect of the NDE1-131A mutant upon NDE1-V5/FLAG-TRAK1 association (Figure 3C, D). In

DOI: 10.1021/acschemneuro.5b00255
ACS Chem. Neurosci. 2016, 7, 553−564

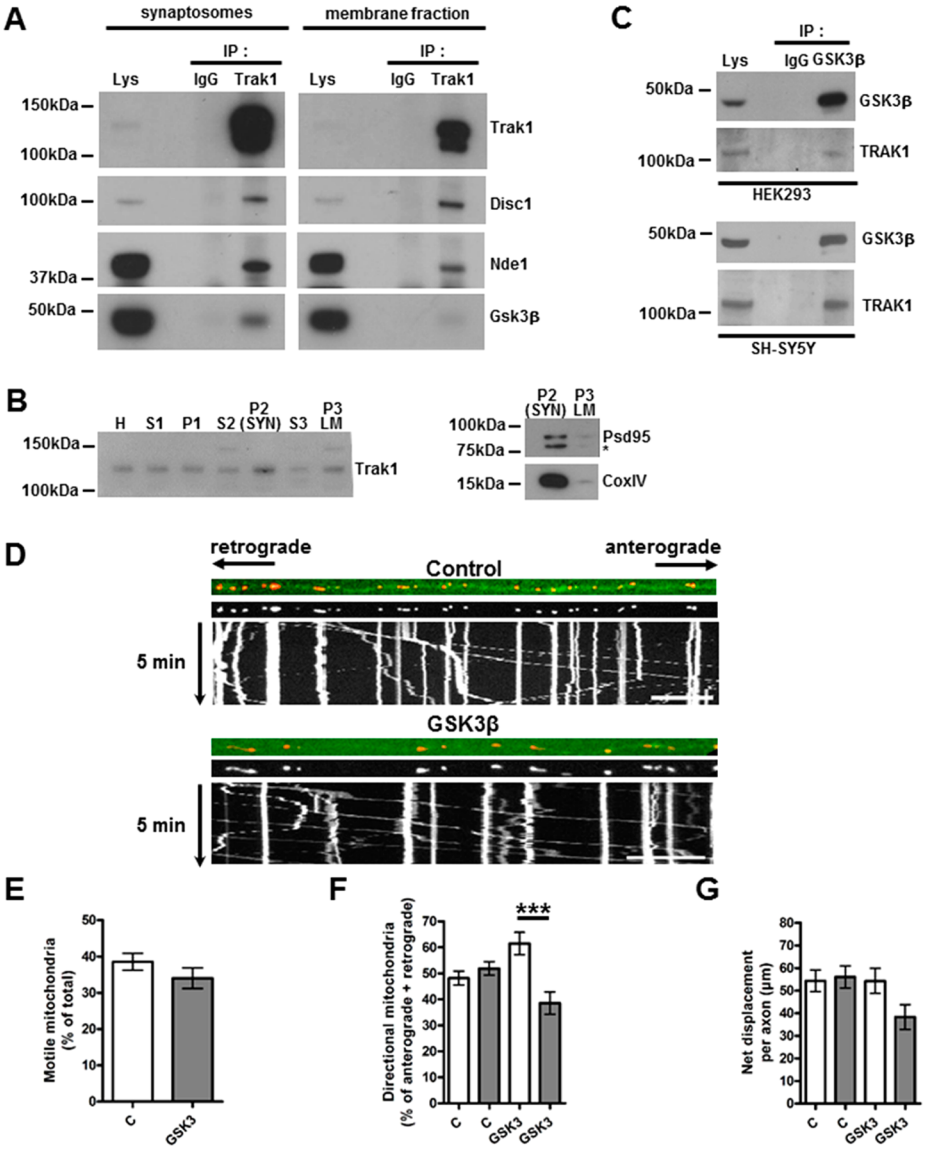

Figure 4. GSK3β associates with TRAK1 and promotes anterograde mitochondrial movement. (A) Immunoprecipitation of Trak1 from adult mouse brain crude synaptosomes (left) or light membrane (right) fractions co-immunoprecipitates Disc1, Nde1, and GSK3β. Trak1 was immunoprecipitated using an antibody from Santa Cruz Biotechnology and detected using an antibody from Sigma-Aldrich. (B) Left: Trak1 is enriched in adult mouse brain crude synaptosome and light membrane fractions. H, homogenate; S1 and P1, supernatant and pellet, respectively, from 1000g centrifugation; S2 and P2 (SYN), supernatant and crude synaptosomes, respectively, from 13 800g centrifugation; S3 and P3 (LM), supernatant and light membranes, respectively, from 100 000g centrifugation. Right: the synaptic marker Psd95 and the mitochondrial marker CoxIV are abundant in the crude synaptosome fraction P2 (SYN), but largely absent from the light membrane fraction P3 (LM). Asterisk (*) indicates a nonspecific band produced by the Psd95 antibody. (C) Immunoprecipitation of human GSK3β from HEK293 (upper) and SH-SY5Y (lower) cell lysates co-immunoprecipitates endogenous TRAK1. Human TRAK1 was detected using an antibody from Sigma. (D) Cultured hippocampal neurons (DIV 6−8) were cotransfected with GFP, DsRed2-mito, and either empty vector or Myc-GSK3β. Time-lapse imaging was performed 1 day post-transfection. Representative images of axons and of kymographs. Scale bars: 20 μm. (E) Mitochondrial motility expressed as percentage of total mitochondria per axon. (F) Motile mitochondria moving in the anterograde (white) or retrograde (dark gray) direction expressed as percentage of anterograde plus retrograde mitochondria per axon. One-way ANOVA $p = 0.002$. (G) Average net displacement per axon of mitochondria moving in the anterograde (white) or retrograde (dark gray) direction. $n = 3$ independent neuronal cultures. One-way ANOVA $p = 0.06$ (not significant), ***$p < 0.0001$.

contrast, the 131E phosphomimic consistently, and substantially, increases NDE1 association with TRAK1 ($p < 0.001$, Figure 3C, D). As previously mentioned, wild-type NDE1-V5 and FLAG-TRAK1 colocalize when exogenously expressed in SH-SY5Y cells (Figure 3E). Colocalization between FLAG-TRAK1 and both NDE1-131A and NDE1-131E is similar to that with wild-type NDE1 (Figure 3E). This suggests that, although the 131E phosphomimic mutation increases TRAK1/NDE1 association, it does not significantly affect association of NDE1 with the trafficking complex. Overall then, NDE1-131E may exert its effects upon mitochondrial movement, at least in part, by altering NDE1 interaction and association with LIS1 and TRAK1 respectively. The purpose of NDE1/TRAK1 association is unknown, but as mentioned earlier, it is likely that NDE1/LIS1 interaction is involved in dynein activation,[18,19,22,23] and this mechanism may therefore be disrupted by the 131E phosphomimic, resulting in reduced dynein activity.

DOI: 10.1021/acschemneuro.5b00255
ACS Chem. Neurosci. 2016, 7, 553−564

Table 2. Numbers of Axons and Mitochondria in Each Category for the GSK3β Mitochondrial Trafficking Experiment

	no. axons	total no	no. stationary	no. motile	no. anterograde	no. retrograde	no. direction undetermined	avg % motility
control	33	970	596	374	180	186	8	39
GSK3β	30	813	522	291	164	121	6	34

We have previously shown that upregulation of cAMP levels reduces NDE1/LIS1 interaction, consistent with the reduced NDE1-131E/LIS1 interaction reported here and previously,[28] We were, however, unable to demonstrate that endogenous NDE1/TRAK1 association is reduced when cAMP signaling is induced by treatment of transfected SH-SY5Y cells with Forskolin to stimulate cAMP synthesis by adenylyl cyclase, plus IBMX to block all cellular cAMP hydrolysis activity by phosphodiesterases (Figure 3F, G). The NDE1-131E mutant therefore does not completely recapitulate the effects of the cAMP signaling system upon the mitochondrial trafficking machinery, at least under the conditions used here. This may be partially due to incomplete phosphorylation of T131 in response to IBMX/Forskolin, consistent with its predicted relative inaccessibility within NDE1 dimers and tetramers.[28] It is also possible that there are other cAMP-dependent phosphorylation sites within the mitochondrial trafficking complex and these could modify the global effect of NDE1 phosphorylation at T131 upon protein−protein interactions/associations within the endogenous complex, resulting in different effects to those seen with exogenous protein pairings.

We next wanted to determine whether another DISC1 interactor that is known to modulate mitochondrial trafficking, GSK3β, is associated with TRAK1. To investigate this, we used a different approach to that used for Trak1/Nde1 (Figure 1A), and immunoprecipitated endogenous mouse Trak1 from mitochondria-containing mouse brain crude synaptosome fractions[31] and from light membrane fractions (Figure 4A). We took this approach because Trak1 protein is enriched in these fractions (Figure 4B). This demonstrated that the Trak1 antibody co-immunoprecipitates mouse Gsk3β along with Disc1 and Nde1, indicating the likely existence of Trak1/Disc1/Nde1/Gsk3β complexes in mouse brain (Figure 4A). Detection of these associations in synaptosomes is consistent with the established presence of mitochondria in this fraction[33] (Figure 4B); however, detection of the associations in the light membrane fraction, where mitochondria are largely absent (Figure 4B), suggests that Trak1 association with Disc1, Nde1, and Gsk3β may not be restricted to mitochondria, consistent with a previous demonstration that Trak1 is involved in endosome-lysosome trafficking[34] as well as mitochondrial trafficking. Additionally, we showed that immunoprecipitation of endogenous human GSK3β from the cell lines HEK293 and SH-SY5Y co-immunoprecipitates endogenous TRAK1 (Figure 4C). GSK3β is therefore another component of the mitochondrial trafficking machinery. As with the TRAK1/NDE1 association, it will be necessary to carry out in vitro binding experiments to determine whether TRAK1 and GSK3β directly interact.

Although GSK3β is already known to regulate mitochondrial trafficking, reports of its effect are conflicting.[24,25] We therefore investigated the effect of overexpressing mouse Gsk3β upon axonal mitochondrial trafficking in cultured hippocampal neurons in our experimental setup. We examined this by transfecting primary mouse hippocampal neurons with Myc-Gsk3β or corresponding empty vector, and carrying out time-lapse imaging of mitochondria within axons over a period of 5 min (Figure 4D, Table 2, and Supporting Information Videos GSK3 Control and GSK3). Gsk3β overexpression does not affect the proportion of motile mitochondria in comparison to empty vector (Figure 4E). However, we did find that Gsk3β promotes anterograde mitochondrial movement, with an average 61% of mitochondria moving in the anterograde direction in axons overexpressing Gsk3β, and only 39% on average moving in the retrograde direction ($p < 0.001$, Figure 4F), with no effect upon mitochondrial displacement (Figure 4G). Thus, in our system at least, Gsk3β overexpression promotes movement of axonal mitochondria in hippocampal neurons in the anterograde direction. A recent study indicates that GSK3β and the NDE1 orthologue NDEL1, synergize to regulate dynein.[35] This study demonstrated that dynein intermediate chain phosphorylation by GSK3β reduces dynein interaction with NDEL1,[35] which would be predicted to reduce dynein activity.[36] Consistent with this prediction, the same study demonstrated that GSK3β inhibition stimulates dynein motility. It is therefore possible that GSK3β also regulates dynein/NDE1 interaction to control dynein activity. Although that study did not specifically investigate mitochondrial motility, since we have now demonstrated association of GSK3β and NDE1 with TRAK1 (Figures 1 and 4A, C), we speculate that this mechanism operates within TRAK1-based mitochondrial trafficking complexes. The increased axonal anterograde mitochondrial movement we observed in response to Gsk3β overexpression (Figure 4F) may therefore occur, at least in part, due to a block on dynein activity as a result of increased dynein intermediate chain phosphorylation, if the tug-of-war hypothesis of bidirectional transport is correct.

Our previous demonstration of (1) a robust association between DISC1 and TRAK1, and (2) promotion of anterograde mitochondrial motility by DISC1, together with all of the above observations, leads us to hypothesize that the molecular scaffold DISC1 and its interactors NDE1 and GSK3β complex with TRAK1 in order to regulate the direction of mitochondrial movement. It is therefore notable that altered expression of, and/or genetic variation in, DISC1, NDE1, and GSK3β, and increased activity of GSK3β, are all implicated in pathogenic mechanisms leading to major mental illness.[14−17,37] We have now demonstrated that altered expression levels of each of these three proteins affects mitochondrial trafficking. The association of these three proteins with the mitochondrial trafficking machinery therefore suggests that defective mitochondrial transport may be a contributory factor in elevated risk of developing psychiatric illness. There is evidence for both neuronal loss[38−42] and mitochondrial abnormalities in psychiatric patients.[1,43] These observations are consistent with our hypothesis that defective mitochondrial trafficking contributes to disease mechanisms in psychiatry: Neurons are particularly sensitive to mitochondrial trafficking defects due to their very high energy requirements and extremely elongated morphology. If mitochondria cannot be efficiently delivered to distant sites throughout the neuron, these sites will be unable to access the mitochondrial functions they require. This could result in neuronal damage and even neuronal death.

Finally, because the NDE1 T131 site that influences mitochondrial trafficking (Figure 2C, D) is phosphorylated by

DOI: 10.1021/acschemneuro.5b00255
ACS Chem. Neurosci. 2016, 7, 553−564

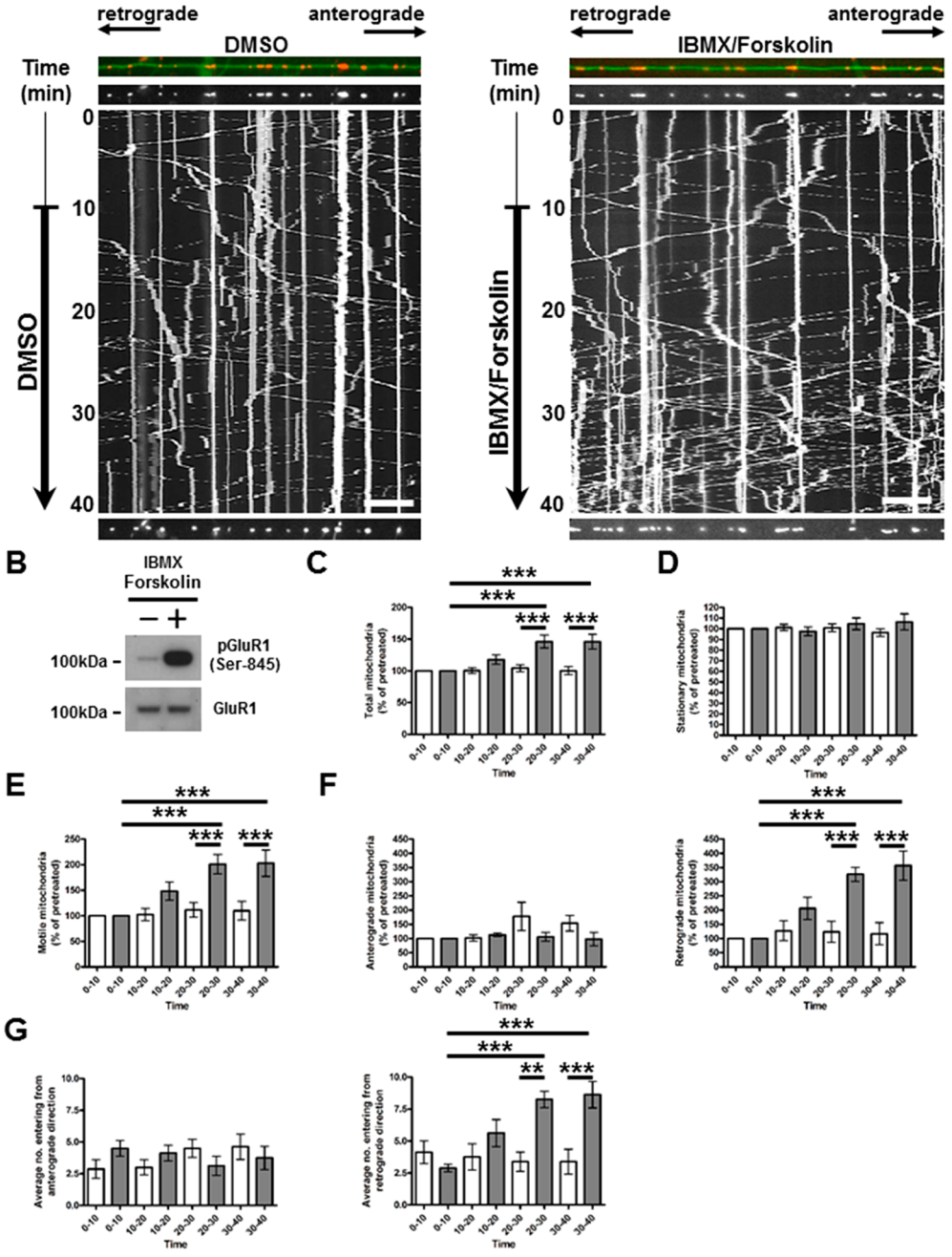

Figure 5. cAMP rapidly promotes retrograde mitochondrial movement within axons of mouse hippocampal neurons. Cultured hippocampal neurons (DIV6–8) were cotransfected with GFP and DsRed2-mito. Time-lapse imaging was performed 1 day post-transfection, with addition of vehicle (DMSO) or 50 μM IBMX plus 50 μM Forskolin 10 min into the imaging period. Scale bars: 20 μm. (A) Representative images of axons and kymographs. Arrows indicate the time of vehicle or drug addition. (B) Phosphorylation of the AMPA receptor subunit GluR1 at the PKA site serine 845 in response to IBMX plus Forskolin treatment of neurons confirms upregulation of cAMP. (C) Total number of mitochondria expressed as percentage of total imaged per axon in the 10 min preceding vehicle (white) or drug (dark gray) addition. One-way ANOVA $p < 0.0001$. (D) Number of stationary mitochondria expressed as percentage of total imaged per axon in the 10 min preceding vehicle (white) or drug (dark gray) addition. (E) Mitochondrial motility expressed as percentage of motile mitochondria imaged per axon in the 10 min preceding vehicle (white) or drug (dark gray) addition. One-way ANOVA $p < 0.0001$. (F) Motile mitochondria moving in the anterograde or retrograde direction expressed as percentage of anterograde or retrograde moving mitochondria imaged per axon in the 10 min preceding vehicle (white) or drug (dark gray) addition. Retrograde mitochondria, one-way ANOVA $p < 0.0001$. (G) Average number of mitochondria entering the imaged axon segment from the anterograde or retrograde direction in neurons treated with vehicle (white) or drug (dark gray). Retrograde mitochondria, one-way ANOVA $p < 0.0001$. $n = 8$ independent neuronal cultures. Error bars represent SEM. $^{**}p < 0.01$, $^{***}p < 0.001$.

the cAMP-dependent kinase PKA,[28] we speculated that mitochondrial trafficking may be regulated by cAMP. The data in Figure 2 predicted that cAMP upregulation should result in T131 phosphorylation and inhibition of retrograde mitochondrial movement, possibly with associated increased anterograde motility. However, the lack of correlation between the effects of 131E and cAMP upregulation upon NDE1/TRAK1 association (Figure 3C, D, F, G) suggested this might not necessarily be the case, possibly because T131 is likely to be relatively inaccessible when NDE1 is fully assembled.[28] We therefore set out to

DOI: 10.1021/acschemneuro.5b00255
ACS Chem. Neurosci. 2016, 7, 553–564

Table 3. Numbers of Axons and Mitochondria in Each Category for the cAMP Mitochondrial Trafficking Experiment

		no. axons	total no.	no. stationary	no. motile	no. anterograde	no. retrograde	no. direction undetermined	avg % motility
0−10 min	DMSO	8	290	150	140	52	84	4	48
	IBMX/Fsk	8	267	149	118	65	50	3	44
10−20 min	DMSO		293	151	142	51	89	2	47
	IBMX/Fsk		313	146	167	72	95	0	53
20−30 min	DMSO		301	151	150	68	79	3	49
	IBMX/Fsk		388	157	231	69	160	2	60
30−40 min	DMSO		288	144	144	67	71	6	49
	IBMX/Fsk		386	157	229	63	165	1	59
total	DMSO		1172	596	576	238	323	15	48
	IBMX/Fsk		1354	609	745	269	470	6	54

examine whether, and how, cAMP levels influence axonal mitochondrial movements. In this experiment, individual axons were imaged for 40 min, with addition of either vehicle (DMSO) or IBMX/Forskolin 10 min into the imaging period, thus allowing 30 min for observation of the effects (Figure 5A, Table 3, Supporting Information Videos DMSO and IBMXFsk). Induction of cAMP signaling by IBMX/Forskolin administration to neuronal cultures was confirmed by substantially increased phosphorylation of the AMPA receptor GluR1 subunit at Serine 845, a site of phosphorylation by PKA (Figure 5B). We found that addition of vehicle had no significant effect upon mitochondrial motility. In striking contrast, IBMX/Forskolin treatment influences mitochondrial movement on several measures, with the effects detectable within 10 min of administration (Figure 5). Induction of cAMP signaling increases the average total number of mitochondria within the imaged axon segments to 118% of pretreated levels within 10 min, and to 146% within 20 min of drug administration ($p < 0.0001$, Figure 5C). This increase is due, at least in part, to elevated numbers of motile mitochondria, with average motility increasing to 148% of pretreated levels within 10 min, and to 201% within 20 min of drug administration ($p < 0.0001$, Figure 5E). The increased motility is apparently entirely due to an increased proportion of mitochondria moving in the retrograde direction, with the average proportion of retrograde mitochondria increasing to 206% of pretreated levels within 10 min of drug addition, and increasing to 326% within 20 min ($p < 0.0001$, Figure 5F). This increase in retrograde mitochondrial motility may be explained, at least in part, by a marked increase in the number of mitochondria entering the imaged axon segment from more distal locations ($p < 0.0001$, Figure 5G). There were no further increases in the following 10 min period, thus the axonal mitochondrial motility response in mouse hippocampal neurons to induction of cAMP signaling apparently peaks within 20 min, and is maintained for at least another 10 min after the plateau is reached. Because (1) the increased numbers of retrograde-moving mitochondria do not correlate with decreased numbers of anterograde-moving mitochondria (Figure 5E) or stationary mitochondria (Figure 5D), but are accompanied by an increase in the total number of mitochondria and increased numbers of moving mitochondria, and (2) measurements were taken, on average, in 155 μm axon segments, 240 μm from the soma, these data indicate that the effect of cAMP is to signal distal mitochondria to move back toward the soma. Although these effects of cAMP upregulation do not recapitulate the mitochondrial motility changes we observed in response to expression of the T131E mutant, they do clearly demonstrate that the cAMP signaling system influences axonal mitochondrial motility. A previous study using rat hippocampal neurons demonstrated that the average speed of mitochondrial movement is influenced by IBMX treatment.[47] IBMX is a nonselective inhibitor of cGMP and cAMP phosphodiesterases, thus the observed alteration in mitochondrial speed generated by IBMX alone, without addition of Forskolin to stimulate cAMP synthesis by adenylyl cyclase, could be due to upregulation of cGMP and/or it could point to velocity as another cAMP-dependent aspect of mitochondrial movement. Multiple aspects of mitochondrial motility may therefore be sensitive to cellular cAMP levels. Nonetheless, the present study shows that directional mitochondrial motility is strongly influenced by cAMP, and the substantial effect suggests that this is an important regulatory mechanism by which mitochondria can rapidly respond to the ever changing needs of the cell.

METHODS

Antibodies. The following antibodies were used in this study. Mouse anti-Myc mAb (9E10, Santa Cruz Biotechnology), goat anti-Myc Ab (Abcam), mouse anti-FLAG M2 mAb (Sigma-Aldrich), rabbit anti-FLAG Ab (Sigma-Aldrich), rabbit anti-NDE1 Ab (Proteintech), rabbit anti-NDE1 Ab EP93,[8] mouse anti-V5 mAb (Invitrogen), goat anti-TRAK1 Ab (Abcam, used to immunoprecipitate and detect human TRAK1), goat anti-Trak1 Ab (Santa Cruz Biotechnology, used to immunoprecipitate mouse Trak1 from mouse brain), rabbit anti-TRAK1 Ab (Sigma-Aldrich, used for human and mouse Trak1 detection on immunoblots), rabbit anti-GluR1 Ab (Santa Cruz Biotechnology), rabbit anti-phospho-GluR1 Ser-845 mAb (Millipore), mouse anti-PSD95 (Invitrogen MA1-046), rabbit anti-COXIV (Abcam), mouse anti-dynactin p150 glued mAb (BD Biosciences), rabbit anti-kinesin-1 Ab (H-50) (Santa Cruz Biotechnology), rabbit anti-GSK3β mAb (27C10, Cell Signaling Technology), and goat anti-LIS1 Ab (Abcam). Endogenous human DISC1 was detected using rabbit anti-human DISC1 C-ter pAb (α-DISC1).[44]

To generate antibodies to mouse Disc1, a C-terminal fragment of mouse Disc1 corresponding to aa 666−852 was bacterially expressed as a GST-fusion protein (GST-mouse Disc1 666−852) and immunized to rabbits to obtain antisera (Eurogentec). The antisera were incubated with GST recombinant protein immobilized on Activated CH-Sepharose 4B beads (GE Healthcare) to adsorb antibodies against GST. This step was repeated to ensure the depletion of anti-GST antibodies in the antisera prior to the final purification of mouse Disc1 antibodies. GST-mouse Disc1 666−852 recombinant protein coupled to activated CH-Sepharose 4B beads was used to purify antimouse Disc1 antibodies from the anti-GST antibodies-depleted antisera. The specificity of this antibody for mouse Disc1 has been previously demonstrated.[30]

Constructs. N-terminal FLAG-tagged human TRAK1 in pcDNA4-TO has been described previously.[7] cDNA fragments encoding C-terminally V5-tagged wild-type or mutant forms of human NDE1 (WT, 131A or 131E) were amplified by PCR using pDEST40 NDE1 constructs[28] as templates, digested with *Bam*HI/NotI restriction enzymes and then inserted into the *Bam*HI/NotI site of pcDNA3.1 to generate pcDNA NDE1-WT-V5, pcDNA NDE1-131A-V5, and pcDNA

DOI: 10.1021/acschemneuro.5b00255
ACS Chem. Neurosci. 2016, 7, 553−564

NDE1-131E-V5, respectively. To generate mouse GSK3β with an N-terminal Myc tag in pcDNA3.1, GSK3β was PCR amplified from mouse cerebellum cDNA, inserted into pcDNA3.1, and fused in-frame to an N-terminal Myc sequence. Sequences of the expression vectors were verified by sequence analysis.

Cell Culture and Transfection. COS7, HEK293, and SH-SY5Y cells were grown in DMEM (Life Technologies) containing 10% fetal bovine serum at 37 °C in 5% CO_2. Hippocampal or cortical neuron cultures were prepared from C57BL/6 mouse fetuses (E17−18) as described previously.[7] For live imaging studies of NDE1-overexpression and IBMX/Forskolin treatment, neuronal cultures were grown on μ-Dishes (Ibidi). For live imaging study of GSK3β overexpression, neurons were grown at low density (1×10^5/well) on 6 well glass bottom plates (In Vitro Scientific) in the presence of an astrocyte feeder layer. Astrocytes were isolated from E18 C57BL/6 mouse cortices as previously described[45] and grown to confluence on culture plate inserts (Millicell) before being used to support neuronal growth. For Western blotting, neurons were grown on a 12 well dish. All dishes and plates used for neuronal culture were coated with poly-D-lysine (Sigma-Aldrich), and neurons were maintained in Neurobasal medium without phenol red (Life Technologies) supplemented with 2% B-27 serum-free supplement (Life Technologies) and 2 mM Glutamax (Life Technologies) at 37 °C in 5% CO_2. Transfection was performed using Lipofectamine 2000 (Life Technologies) according to the manufacturer's instructions. At 20−24 h post-transfection, cells were harvested for co-immunoprecipitation experiments or live imaging.

DISC1 Knockdown. DISC1 knockdown in human cell lines was performed as described previously.[7] Silencer Select Negative Control siRNA and human DISC1 siRNAs [Silencer Select siRNA DISC1 #2 (targeting exon 13), Silencer Select siRNA DISC1 #5 (targeting exon 2)] were purchased from Ambion. HEK293 or SH-SY5Y cells were transfected with control or DISC1 siRNA at a final concentration of 50 nM using Lipofectamine 2000. Cells were harvested for co-immunoprecipitation assays or Western blotting 48 h post-transfection.

Reverse Transcriptase PCR. HEK293 RNA was prepared using the Qiagen RNeasy extraction kit. HEK293 and human brain cDNA (from human brain total RNA, AM7962, ThermoFisher Scientific) were prepared using the First Strand cDNA synthesis kit (Roche) according to the manufacturer's instructions. PCR to detect *TRAK1* transcripts was carried out using Taq DNA polymerase (Sigma-Aldrich) and cycled using a touchdown PCR program as follows: [95 °C 2 min] × 1 cycle, [95 °C 20 s, 65 °C 30 s (−1 °C/cycle), 72 °C 1 min] × 10 cycles followed by [95 °C 20 s, 55 °C 30 s, 72 °C 1 min] × 30 cycles, [72 °C 10 min] × 1 cycle. Products were resolved using standard agarose gel electrophoresis. Primers sequences were ggaggacaagtacgcagagt (TRAK1 exon 10) and gttcatgggagaaggggtca (TRAK1 exon 12).

PCR products were treated with ExoSAP-IT (GE healthcare) prior to direct sequencing. BigDye Terminator sequencing of PCR products was carried out using 1 μL of BDv3.1, 1.5 μL of 5× sequencing buffer, 1 μL of DNA template, and 6 μL of dH_2O. Reactions were cycled as follows: 96 °C, 1 min (1 cycle); 96 °C, 10 s, 50 °C, 5 s, 60 °C-4 min (25 cycles); 4 °C hold. Sequencing chromatograms were analyzed using Chromas (version 1.45).

Subcellular Fractionation of Mouse Brain. Crude synaptosomes and light membrane fractions were prepared as described previously.[46] Briefly, C57BL/6 adult mouse brains were homogenized in a sucrose buffer solution [1 mM HEPES (pH7.5), 0.32 M sucrose, 1 mM $NaHCO_3$, 1 mM $MgCl_2$ Complete Mini Protease Inhibitor Tablet (Roche), and Phosphatase Inhibitor Cocktail Set II (Calbiochem)] using a dounce tissue grinder. The S1 supernatant was obtained by centrifugation of the homogenates at 1000*g* for 10 min and further fractionated into the S2 supernatant and the P2 crude synaptosomal pellets by centrifugation at 13 800*g* for 10 min. To obtain the light membrane P3 pellets, the S2 supernatant was centrifuged at 100 000*g* for 1 h (Beckman TLA 100.3). Each fraction was harvested for co-immunoprecipitation assays.

Co-Immunoprecipitation. Cultured cells were lysed in IP buffer [1% Triton X-100, with/without 0.1% SDS, 50 mM Tris−HCl (pH 7.5), 150 mM NaCl, Complete Mini Protease Inhibitor Tablet (Roche), Phosphatase Inhibitor Cocktail Set II (Calbiochem)]. Insoluble materials were removed by centrifugation at 100 000*g*. C57BL/6 adult mouse brains or crude synaptosomes/light membrane pellets were lysed in IP buffer, and insoluble materials were removed by ultracentrifugation at 100 000*g* (Beckman TLA 100.3) for 30 min at 4 °C. Cell lysates were precleared with protein G-Sepharose beads (Sigma) alone for 1 h at 4 °C, and then incubated with appropriate antibodies overnight at 4 °C with rotation. Protein G-Sepharose beads were added to the lysates and further incubated for 2 h. Immune complexes on the beads were washed with IP buffer three times and with 50 mM Tris−HCl (pH 7.5) once. Bound proteins were eluted with SDS loading buffer and analyzed by Western blotting.

Western Blot Analysis. Protein samples were separated by SDS-PAGE using NuPAGE 4−12% gels (Invitrogen), transferred onto PVDF membranes (GE Healthcare) using Trans-Blot SD Semi-Dry Transfer Cell (Bio-Rad), and blocked in 1% skimmed milk in T-TBS [50 mM Tris−HCl (pH 7.5), 150 mM NaCl, and 0.1% Tween-20] at room temperature (RT). Incubation with primary antibodies was performed overnight at 4 °C. Blots were incubated with horseradish peroxidase-conjugated secondary antibodies [Rabbit antimouse IgG HRP, Swine antirabbit IgG HRP or Rabbit antigoat IgG HRP (DAKO)] for 45 min at RT and then protein bands were visualized by ECL or ECL-2 Western blotting substrate (Thermo Scientific). Some blots were stripped with Restore PLUS Western Blot Stripping Buffer (Thermo Scientific) and reprobed with appropriate antibodies. Relative intensities of protein bands were quantified with ImageJ densitometry analysis.

Immunocytochemistry. SH-SY5Y cells were transfected with V5-tagged NDE1 plus FLAG-tagged TRAK1 expression constructs. Cells were fixed in 4% paraformaldehyde for 10 min at room temperature followed by permeabilisation with 0.2% Triton X-100 for 10 min. Fixed cells were blocked in phosphate-buffered saline containing 3% bovine serum albumin and incubated with primary or secondary antibodies diluted in 3% bovine serum albumin for 1 h at room temperature. Rabbit anti-NDE1 (Proteintech) was diluted at 1:500 and mouse anti-FLAG was diluted at 1:10 000. Alexa Fluor 488 goat anti-rabbit and Alexa Fluor 594 chicken anti-mouse were used as secondary antibodies. Nuclei were visualized with Hoechst stain. Confocal images were acquired using a Nikon Eclipse Ti confocal microscope with a Plan-Apochromat 100× objective lens.

Live Cell Imaging. Time-lapse imaging of mitochondria in axons was conducted as described previously.[7] In brief, C57BL/6 mouse hippocampal neurons were cotransfected with pMax-GFP, pDsRed2-mito and pcDNA3.1 NDE1 constructs (either empty vector, NDE1-WT-V5, T131A-V5, or T131E) in a 1:1:4 ratio (DIV 6−7 neurons), or with pcDNA3.1 empty vector or pcDNA3.1 Myc-GSK3β in a 1:4:5 ratio (DIV 6−8 neurons). To examine effects of IBMX/Forskolin-treatment on mitochondrial motility, hippocampal neurons at DIV6−8 were cotransfected with pMax-GFP and pDsRed2-mito. At 20−24 h after transfection, live imaging was performed in a climate-controlled chamber at 37 °C in 5% CO_2. Images of DsRed2-mito-labeled axonal mitochondria were captured with a Photometrics Evolve EMCCD camera on a Nikon C1SI/TiE microscope equipped with a Plan-Fluor 40×/0.75 OFN25 DIC objective plus an additional ×1.5 optical lens (×60 total). Images were acquired every 2 s for 3 min (for effects of NDE1 expression on mitochondrial motility), every 3 s for 5 min (for effects of GSK3β expression) or every 4 s for 40 min (for effects of IBMX/Forskolin stimuli) and then kymographs were created with NIS Elements (Nikon).

Axonal segments selected for recording were at least 100 μm away from the cell soma. Average length of the axonal sections and average distance from the cell soma are as follows. For effects of NDE1 expression: [average distance from the cell soma (control n = 26; 173.1 μm ± 11.6, NDE1-WT, n = 27; 226.0 μm ± 20.1, NDE1-T131A, n = 28; 204.1 μm ± 13.5, NDE1-T131E, n = 27; 206.5 μm ± 14.3)], [average length of the axonal sections (control n = 26; 161.9 μm ± 4.9, NDE1-WT, n = 27; 154.6 μm ± 4.7, NDE1-T131A, n = 28; 162.0 μm ± 3.2, NDE1-T131E, n = 27; 169.0 μm ± 4.4)]. For effects of Gsk3β expression: [average distance from the cell soma (control n = 33:156.1 μm ± 8.9, Gsk3β n = 30; 156.0 ± 8.4], [average length of the axonal sections (control n = 33; 168.3 μm ± 6.2, Gsk3β n = 30; 162.9 ± 4.5]. For effects of IBMX/Forskolin stimulation: [average distance from the

DOI: 10.1021/acschemneuro.5b00255
ACS Chem. Neurosci. 2016, 7, 553−564

cell soma (control $n = 8$; 240.2 μm ± 38.8, IBMX/Forskolin $n = 8$; 240.3 μm ± 39.5)], [average length of the axonal sections (control $n = 8$; 154.6 μm ± 6.6, IBMX/Fsk $n = 8$; 158.2 μm ± 5.5)].

To stimulate hippocampal neurons with Forskolin and IBMX, 1 mL of Neurobasal medium + B27/Glutamax containing 100 μM Forskolin (Tocris) plus 100 μM IBMX (Tocris) was freshly prepared approximately 5 min beforehand. After 10 min of imaging mitochondrial motility under basal conditions, the IBMX/Forskolin-containing medium was added directly to the existing 1 mL of culture medium, avoiding any disturbance during imaging. The final concentrations of both Forskolin and IBMX were 50 μM in 2 mL of culture medium. Transfection with expression constructs and subsequent live imaging was conducted in a blinded fashion. Motile mitochondria were defined as those which traveled more than 3 μm within 3 min. Motile mitochondria that were not classed as anterograde or retrograde either were oscillating or their overall direction of movement could not be determined. Displacement measurements were not determined using data obtained from the IBMX/Forskolin experiments because accurate measurements were precluded by the high density of motile mitochondria on the kymographs.

Statistical Analysis. GraphPad Prism software was used for data analysis. Data were analyzed using one-way ANOVA with pairwise Bonferroni post-testing. All values are presented as mean ± SEM.

■ ASSOCIATED CONTENT

Supporting Information

The Supporting Information is available free of charge on the ACS Publications website at DOI: 10.1021/acschemneuro.5b00255. In the NDE1 and GSK3β videos, 1 s is equivalent to 30 s of real time. In the cAMP videos, 1 s is equivalent to 1 min of real time.

Representative example of time-lapse imaging of hippocampal neuronal axons treated with DMSO (DMSO) (AVI)

Representative examples of time-lapse imaging of hippocampal neuronal axons treated treated with IBMX plus Forskolin to upregulate cAMP (IBMXFsk) (AVI)

Representative examples of time-lapse imaging of hippocampal neuronal axons transfected with GSK3β (GSK3) (AVI)

Representative examples of time-lapse imaging of hippocampal neuronal axons transfected with empty vector, GSK3 control (GSK3 Control) (AVI)

Representative examples of time-lapse imaging of hippocampal neuronal axons transfected with empty vector, NDE1 control (NDE1 Control) (AVI)

Representative examples of time-lapse imaging of hippocampal neuronal axons transfected with phosphomutant NDE1 (NDE1-131A) (AVI)

Representative examples of time-lapse imaging of hippocampal neuronal axons transfected with phosphomimic NDE1 (NDE1-131E) (AVI)

Representative examples of time-lapse imaging of hippocampal neuronal axons transfected with wild-type NDE1 (NDE1-WT) (AVI)

■ AUTHOR INFORMATION

Corresponding Author

*Telephone: (+44) 131 651 8732. Fax: (+44) 131 651 1059. E-mail: Kirsty.millar@ed.ac.uk.

Present Address

†F.O.: Department of Immunology, Juntendo University School of Medicine, 2-1-1 Hongo, Bunkyo-ku, Tokyo 113-8421, Japan

Author Contributions

Participated in research design: F.O., L.C.M., E.L.V.M., and J.K.M. Conducted experiments: F.O., L.C.M., S.T.O'S., and H.S.T. Performed data analysis: F.O., L.C.M., E.L.V.M., and J.K.M. Wrote manuscript: F.O., D.J.P., and J.K.M.

Funding

This work was funded by the Medical Research Council (MRC Project Grant G0902166), an MRC-funded IGMM studentship awarded to L.C.M., and the Wellcome Trust-University of Edinburgh Institutional Strategic Support Fund.

Notes

The authors declare no competing financial interest.

■ ACKNOWLEDGMENTS

We thank Matthew Pearson and Ann Wheeler for technical assistance with live cell imaging.

■ REFERENCES

(1) Manji, H., Kato, T., Di Prospero, N. A., Ness, S., Beal, M. F., Krams, M., and Chen, G. (2012) Impaired mitochondrial function in psychiatric disorders. *Nat. Rev. Neurosci. 13*, 293−307.

(2) Schwarz, T. L. (2013) Mitochondrial trafficking in neurons. *Cold Spring Harbor Perspect. Biol. 5*, a011304.

(3) Brickley, K., and Stephenson, F. A. (2011) Trafficking kinesin protein (TRAK)-mediated transport of mitochondria in axons of hippocampal neurons. *J. Biol. Chem. 286*, 18079−18092.

(4) Brickley, K., Smith, M. J., Beck, M., and Stephenson, F. A. (2005) GRIF-1 and OIP106, members of a novel gene family of coiled-coil domain proteins: association in vivo and in vitro with kinesin. *J. Biol. Chem. 280*, 14723−14732.

(5) van Spronsen, M., Mikhaylova, M., Lipka, J., Schlager, M. A., van den Heuvel, D. J., Kuijpers, M., Wulf, P. S., Keijzer, N., Demmers, J., Kapitein, L. C., Jaarsma, D., Gerritsen, H. C., Akhmanova, A., and Hoogenraad, C. C. (2013) TRAK/Milton Motor-Adaptor Proteins Steer Mitochondrial Trafficking to Axons and Dendrites. *Neuron 77*, 485−502.

(6) Brickley, K., Pozo, K., and Stephenson, F. A. (2011) N-acetylglucosamine transferase is an integral component of a kinesin-directed mitochondrial trafficking complex. *Biochim. Biophys. Acta, Mol. Cell Res. 1813*, 269−281.

(7) Ogawa, F., Malavasi, E. L., Crummie, D. K., Eykelenboom, J. E., Soares, D. C., Mackie, S., Porteous, D. J., and Millar, J. K. (2014) DISC1 complexes with TRAK1 and Miro1 to modulate anterograde axonal mitochondrial trafficking. *Hum. Mol. Genet. 23*, 906−919.

(8) Bradshaw, N. J., Christie, S., Soares, D. C., Carlyle, B. C., Porteous, D. J., and Millar, J. K. (2009) NDE1 and NDEL1: multimerisation, alternate splicing and DISC1 interaction. *Neurosci. Lett. 449*, 228−233.

(9) Brandon, N. J., Handford, E. J., Schurov, I., Rain, J. C., Pelling, M., Duran-Jimeniz, B., Camargo, L. M., Oliver, K. R., Beher, D., Shearman, M. S., and Whiting, P. J. (2004) Disrupted in Schizophrenia 1 and Nudel form a neurodevelopmentally regulated protein complex: implications for schizophrenia and other major neurological disorders. *Mol. Cell. Neurosci. 25*, 42−55.

(10) Ozeki, Y., Tomoda, T., Kleiderlein, J., Kamiya, A., Bord, L., Fujii, K., Okawa, M., Yamada, N., Hatten, M. E., Snyder, S. H., Ross, C. A., and Sawa, A. (2003) Disrupted-in-Schizophrenia-1 (DISC-1): mutant truncation prevents binding to NudE-like (NUDEL) and inhibits neurite outgrowth. *Proc. Natl. Acad. Sci. U. S. A. 100*, 289−294.

(11) Mao, Y., Ge, X., Frank, C. L., Madison, J. M., Koehler, A. N., Doud, M. K., Tassa, C., Berry, E. M., Soda, T., Singh, K. K., Biechele, T., Petryshen, T. L., Moon, R. T., Haggarty, S. J., and Tsai, L. H. (2009) Disrupted in schizophrenia 1 regulates neuronal progenitor proliferation via modulation of GSK3beta/beta-catenin signaling. *Cell 136*, 1017−1031.

(12) Millar, J. K., Wilson-Annan, J. C., Anderson, S., Christie, S., Taylor, M. S., Semple, C. A., Devon, R. S., St Clair, D. M., Muir, W. J., Blackwood, D. H., and Porteous, D. J. (2000) Disruption of two novel

DOI: 10.1021/acschemneuro.5b00255
ACS Chem. Neurosci. 2016, 7, 553−564

genes by a translocation co-segregating with schizophrenia. *Hum. Mol. Genet. 9*, 1415−1423.
(13) Blackwood, D. H., Fordyce, A., Walker, M. T., St. Clair, D. M., Porteous, D. J., and Muir, W. J. (2001) Schizophrenia and affective disorders–cosegregation with a translocation at chromosome 1q42 that directly disrupts brain-expressed genes: clinical and P300 findings in a family. *Am. J. Hum. Genet. 69*, 428−433.
(14) Malhotra, D., and Sebat, J. (2012) CNVs: harbingers of a rare variant revolution in psychiatric genetics. *Cell 148*, 1223−1241.
(15) Jope, R. S., and Roh, M. S. (2006) Glycogen synthase kinase-3 (GSK3) in psychiatric diseases and therapeutic interventions. *Curr. Drug Targets 7*, 1421−1434.
(16) Emamian, E. S. (2012) AKT/GSK3 signaling pathway and schizophrenia. *Front. Mol. Neurosci. 5*, 33.
(17) Ronai, Z., Kovacs-Nagy, R., Szantai, E., Elek, Z., Sasvari-Szekely, M., Faludi, G., Benkovits, J., Rethelyi, J. M., and Szekely, A. (2014) Glycogen synthase kinase 3 beta gene structural variants as possible risk factors of bipolar depression. *Am. J. Med. Genet., Part B 165B*, 217−222.
(18) Li, J., Lee, W. L., and Cooper, J. A. (2005) NudEL targets dynein to microtubule ends through LIS1. *Nat. Cell Biol. 7*, 686−690.
(19) McKenney, R. J., Vershinin, M., Kunwar, A., Vallee, R. B., and Gross, S. P. (2010) LIS1 and NudE induce a persistent dynein force-producing state. *Cell 141*, 304−314.
(20) Reiner, O., and Sapir, T. (2013) LIS1 functions in normal development and disease. *Curr. Opin. Neurobiol. 23*, 951−956.
(21) Shao, C. Y., Zhu, J., Xie, Y. J., Wang, Z., Wang, Y. N., Wang, Y., Su, L. D., Zhou, L., Zhou, T. H., and Shen, Y. (2013) Distinct functions of nuclear distribution proteins LIS1, Ndel1 and NudCL in regulating axonal mitochondrial transport. *Traffic 14*, 785−797.
(22) Liang, Y., Yu, W., Li, Y., Yang, Z., Yan, X., Huang, Q., and Zhu, X. (2004) Nudel functions in membrane traffic mainly through association with Lis1 and cytoplasmic dynein. *J. Cell Biol. 164*, 557−566.
(23) Yan, X., Li, F., Liang, Y., Shen, Y., Zhao, X., Huang, Q., and Zhu, X. (2003) Human Nudel and NudE as regulators of cytoplasmic dynein in poleward protein transport along the mitotic spindle. *Mol. Cell. Biol. 23*, 1239−1250.
(24) Chen, S., Owens, G. C., Crossin, K. L., and Edelman, D. B. (2007) Serotonin stimulates mitochondrial transport in hippocampal neurons. *Mol. Cell. Neurosci. 36*, 472−483.
(25) Llorens-Martin, M., Lopez-Domenech, G., Soriano, E., and Avila, J. (2011) GSK3beta is involved in the relief of mitochondria pausing in a Tau-dependent manner. *PLoS One 6*, e27686.
(26) Chen, S., Owens, G. C., Makarenkova, H., and Edelman, D. B. (2010) HDAC6 regulates mitochondrial transport in hippocampal neurons. *PLoS One 5*, e10848.
(27) Reed, N. A., Cai, D., Blasius, T. L., Jih, G. T., Meyhofer, E., Gaertig, J., and Verhey, K. J. (2006) Microtubule acetylation promotes kinesin-1 binding and transport. *Curr. Biol. 16*, 2166−2172.
(28) Bradshaw, N. J., Soares, D. C., Carlyle, B. C., Ogawa, F., Davidson-Smith, H., Christie, S., Mackie, S., Thomson, P. A., Porteous, D. J., and Millar, J. K. (2011) PKA phosphorylation of NDE1 is DISC1/PDE4 dependent and modulates its interaction with LIS1 and NDEL1. *J. Neurosci. 31*, 9043−9054.
(29) Kuroda, K., Yamada, S., Tanaka, M., Iizuka, M., Yano, H., Mori, D., Tsuboi, D., Nishioka, T., Namba, T., Iizuka, Y., Kubota, S., Nagai, T., Ibi, D., Wang, R., Enomoto, A., Isotani-Sakakibara, M., Asai, N., Kimura, K., Kiyonari, H., Abe, T., Mizoguchi, A., Sokabe, M., Takahashi, M., Yamada, K., and Kaibuchi, K. (2011) Behavioral alterations associated with targeted disruption of exons 2 and 3 of the Disc1 gene in the mouse. *Hum. Mol. Genet. 20*, 4666−4683.
(30) Chandran, J. S., Kazanis, I., Clapcote, S. J., Ogawa, F., Millar, J. K., Porteous, D. J., and Ffrench-Constant, C. (2014) Disc1 variation leads to specific alterations in adult neurogenesis. *PLoS One 9*, e108088.
(31) Ueda, T., Greengard, P., Berzins, K., Cohen, R. S., Blomberg, F., Grab, D. J., and Siekevitz, P. (1979) Subcellular distribution in cerebral cortex of two proteins phosphorylated by a cAMP-dependent protein kinase. *J. Cell Biol. 83*, 308−319.
(32) Atkin, T. A., MacAskill, A. F., Brandon, N. J., and Kittler, J. T. (2011) Disrupted in Schizophrenia-1 regulates intracellular trafficking of mitochondria in neurons. *Mol. Psychiatry 16*, 122−124.
(33) Deutsch, C., Drown, C., Rafalowska, U., and Silver, I. A. (1981) Synaptosomes from rat brain: morphology, compartmentation, and transmembrane pH and elctrical gradients. *J. Neurochem. 36*, 2063−2072.
(34) Webber, E., Li, L., and Chin, L. S. (2008) Hypertonia-associated protein Trak1 is a novel regulator of endosome-to-lysosome trafficking. *J. Mol. Biol. 382*, 638−651.
(35) Gao, F. J., Hebbar, S., Gao, X. A., Alexander, M., Pandey, J. P., Walla, M. D., Cotham, W. E., King, S. J., and Smith, D. S. (2015) GSK-3beta Phosphorylation of Cytoplasmic Dynein Reduces Ndel1 Binding to Intermediate Chains and Alters Dynein Motility. *Traffic 16*, 941−61.
(36) Vallee, R. B., McKenney, R. J., and Ori-McKenney, K. M. (2012) Multiple modes of cytoplasmic dynein regulation. *Nat. Cell Biol. 14*, 224−230.
(37) Millar, J. K., Pickard, B. S., Mackie, S., James, R., Christie, S., Buchanan, S. R., Malloy, M. P., Chubb, J. E., Huston, E., Baillie, G. S., Thomson, P. A., Hill, E. V., Brandon, N. J., Rain, J. C., Camargo, L. M., Whiting, P. J., Houslay, M. D., Blackwood, D. H., Muir, W. J., and Porteous, D. J. (2005) DISC1 and PDE4B are interacting genetic factors in schizophrenia that regulate cAMP signaling. *Science 310*, 1187−1191.
(38) Vita, A., De Peri, L., Deste, G., and Sacchetti, E. (2012) Progressive loss of cortical gray matter in schizophrenia: a meta-analysis and meta-regression of longitudinal MRI studies. *Transl. Psychiatry 2*, e190.
(39) Van Haren, N. E., Cahn, W., Hulshoff Pol, H. E., and Kahn, R. S. (2013) Confounders of excessive brain volume loss in schizophrenia. *Neurosci. Biobehav. Rev. 37*, 2418−2423.
(40) Fraguas, D., Diaz-Caneja, C. M., Pina-Camacho, L., Janssen, J., and Arango, C. (2014) Progressive brain changes in children and adolescents with early-onset psychosis: A meta-analysis of longitudinal MRI studies. *Schizophr. Res.*, DOI: 10.1016/j.schres.2014.12.022.
(41) Gupta, C. N., Calhoun, V. D., Rachakonda, S., Chen, J., Patel, V., Liu, J., Segall, J., Franke, B., Zwiers, M. P., Arias-Vasquez, A., Buitelaar, J., Fisher, S. E., Fernandez, G., van Erp, T. G., Potkin, S., Ford, J., Mathalon, D., McEwen, S., Lee, H. J., Mueller, B. A., Greve, D. N., Andreassen, O., Agartz, I., Gollub, R. L., Sponheim, S. R., Ehrlich, S., Wang, L., Pearlson, G., Glahn, D. C., Sprooten, E., Mayer, A. R., Stephen, J., Jung, R. E., Canive, J., Bustillo, J., and Turner, J. A. (2015) Patterns of Gray Matter Abnormalities in Schizophrenia Based on an International Mega-analysis. *Schiz. Bull. 41*, 1133−42.
(42) Cannon, T. D., Chung, Y., He, G., Sun, D., Jacobson, A., van Erp, T. G., McEwen, S., Addington, J., Bearden, C. E., Cadenhead, K., Cornblatt, B., Mathalon, D. H., McGlashan, T., Perkins, D., Jeffries, C., Seidman, L. J., Tsuang, M., Walker, E., Woods, S. W., and Heinssen, R. (2015) Progressive reduction in cortical thickness as psychosis develops: a multisite longitudinal neuroimaging study of youth at elevated clinical risk. *Biol. Psychiatry 77*, 147−157.
(43) Popa-Wagner, A., Mitran, S., Sivanesan, S., Chang, E., and Buga, A. M. (2013) ROS and brain diseases: the good, the bad, and the ugly. *Oxid. Med. Cell. Longevity 2013*, 963520.
(44) Ogawa, F., Kasai, M., and Akiyama, T. (2005) A functional link between Disrupted-In-Schizophrenia 1 and the eukaryotic translation initiation factor 3. *Biochem. Biophys. Res. Commun. 338*, 771−776.
(45) Kaech, S., and Banker, G. (2006) Culturing hippocampal neurons. *Nat. Protoc. 1*, 2406−2415.
(46) Clapcote, S. J., Lipina, T. V., Millar, J. K., Mackie, S., Christie, S., Ogawa, F., Lerch, J. P., Trimble, K., Uchiyama, M., Sakuraba, Y., Kaneda, H., Shiroishi, T., Houslay, M. D., Henkelman, R. M., Sled, J. G., Gondo, Y., Porteous, D. J., and Roder, J. C. (2007) Behavioral phenotypes of Disc1 missense mutations in mice. *Neuron 54*, 387−402.
(47) Chen, S., Owens, G. C., and Edelman, B. B. (2008) Dopamine inhibits mitochondrial motility in hippocampal neurons. *PLoS One 3*, e2804.

DOI: 10.1021/acschemneuro.5b00255
ACS Chem. Neurosci. 2016, 7, 553−564